

## New $\tau$ Physics Results from ARGUS

Bernhard Spaan\*

*Institut für Physik, Universität Dortmund, 4600 Dortmund 50, Germany*

### Abstract

New results from ARGUS on  $\tau$  physics are presented: the measurement of the  $\tau$  mass and the measurement of the decay  $\tau^- \rightarrow \rho^- \nu_\tau$ . The implications on lepton universality,  $\nu_\tau$  mass, structure of the weak interaction and the  $\nu_\tau$  spin will be discussed.

### Introduction

A rich field of physics is accessible to detectors taking data at  $e^+e^-$  storage rings which operate in the center-of-mass energy range corresponding to the  $\Upsilon$  resonance masses (DORIS II, CESR). A large fraction of the research efforts is devoted to the study of the  $\tau$  lepton and its associated neutrino,  $\nu_\tau$ .

The detector ARGUS at the DORIS II storage ring started to contribute to the field of  $\tau$  physics as early as 1985. Since then, a large number of analyses have been performed. In this article I report in detail on two recent measurements: 1) the measurement of the  $\tau$  mass and 2) the measurement of the decay  $\tau^- \rightarrow \rho^- \nu_\tau$ .<sup>†</sup> In addition, I report briefly on three other recent measurements:

1. The search for neutrinoless  $\tau$  decays. Upper limits on branching ratios for six neutrinoless leptonic, 16 semileptonic, two radiative-leptonic, two radiative-hadronic and three purely hadronic  $\tau$  decays have been determined.<sup>1</sup> The results are listed in Table 1 where they are compared to previous measurements.
2. Measurement of exclusive one-prong branching ratios:  $B_e = (17.3 \pm 0.4 \pm 0.5)\%$ ,  $B_\mu = (17.2 \pm 0.4 \pm 0.5)\%$  and  $B_h = (11.7 \pm 0.6 \pm 0.8)\%$ .<sup>8</sup> The topological three-prong branching ratio  $B_3$  has been extracted using the leptonic decays as reference:  $B_3 = (13.3 \pm 0.3 \pm 0.8)\%$ .
3. The measurement of the decay  $\tau^- \rightarrow \pi^+\pi^+\pi^-\nu_\tau$ .<sup>7</sup> The  $\tau$  decay into three charged pions is dominantly mediated by the decay  $\tau^- \rightarrow a_1^- \nu_\tau$  with the

\*Representing the ARGUS Collaboration; supported by the German Bundesministerium für Forschung und Technologie under contract number 054DO51P.

<sup>†</sup>References in this article to a specific charged state also imply the charge conjugate state.

Decay Channel	MARK II	ARGUS 86	Crystal Ball	CLEO	ARGUS 91
$\tau^- \rightarrow e^- e^+ e^-$	40	3.8		3.0	1.3
$\tau^- \rightarrow e^- \mu^+ \mu^-$	33	3.3		2.7	1.9
$\tau^- \rightarrow e^+ \mu^- \mu^-$				1.6	1.8
$\tau^- \rightarrow \mu^- e^+ e^-$	44	3.3		2.7	1.4
$\tau^- \rightarrow \mu^+ e^- e^-$				1.6	1.4
$\tau^- \rightarrow \mu^- \mu^+ \mu^-$	49	2.9		1.7	1.9
$\tau^- \rightarrow e^- \pi^+ \pi^-$		4.2		6.0	2.7
$\tau^- \rightarrow e^+ \pi^- \pi^-$				1.7	1.8
$\tau^- \rightarrow \mu^- \pi^+ \pi^-$		4.0		3.9	3.6
$\tau^- \rightarrow \mu^+ \pi^- \pi^-$					6.3
$\tau^- \rightarrow e^- \rho^0$	37	3.9			1.9
$\tau^- \rightarrow \mu^- \rho^0$	44	3.8			2.9
$\tau^- \rightarrow e^- \pi^+ K^-$		4.2		5.8	2.9
$\tau^- \rightarrow e^+ \pi^- K^-$				4.9	2.0
$\tau^- \rightarrow \mu^- \pi^+ K^-$		12		7.7	11
$\tau^- \rightarrow \mu^+ \pi^- K^-$				4.0	5.8
$\tau^- \rightarrow e^- K^{*0}$	130	5.4			3.8
$\tau^- \rightarrow \mu^- K^{*0}$	100	5.9			4.5
$\tau^- \rightarrow e^- \gamma$	64		20		12
$\tau^- \rightarrow e^- \pi^0$	210		14		17
$\tau^- \rightarrow \mu^- \gamma$	55				3.4
$\tau^- \rightarrow \mu^- \pi^0$	82				4.4
$\tau^- \rightarrow e^- \eta$			24		6.3
$\tau^- \rightarrow \mu^- \eta$					7.3
$\tau^- \rightarrow \bar{p} \gamma$					29
$\tau^- \rightarrow \bar{p} \pi^0$					65.5
$\tau^- \rightarrow \pi^- \gamma$					28
$\tau^- \rightarrow \pi^- \pi^0$					37
$\tau^- \rightarrow \bar{p} \eta$					129

Table 1: Upper limits [ $10^{-5}$ ] (90% CL) on branching ratios of neutrinoless  $\tau$  decays compared with results from previous experiments.<sup>2-5</sup>

subsequent decays  $a_1^- \rightarrow \rho^0 \pi^-$  and  $\rho^0 \rightarrow \pi^+ \pi^-$ . Using the model of Isgur et al.,<sup>8</sup> the parameters of the  $a_1$  have been determined to be  $m(a_1) = (1.211 \pm 0.007 \pm_{0.050}^{0.050}) \text{ GeV}/c^2$  and  $\Gamma_{a_1} = (0.446 \pm 0.021 \pm_{0.140}^{0.140}) \text{ GeV}/c^2$ . The second errors reflect the model dependence of the result. This is the currently most significant determination of the  $a_1$  resonance parameters. The ratio of S- and D-wave amplitudes for the  $\rho^0 \pi^-$  intermediate state of the  $a_1^-$  decay at the nominal  $a_1^-$  mass was found to be  $D/S = -0.11 \pm 0.02$ . Using this D/S ratio we update our former measurement<sup>9</sup> of the parity violating asymmetry parameter  $\gamma_{AV} = 2g_A g_V / (g_A^2 + g_V^2)$  to be  $1.25 \pm 0.23 \pm_{0.08}^{0.15}$ .

### Measurement of the $\tau$ mass

As early as 1984 it has been noticed that the sum of all measured exclusive  $\tau$  branching ratios is significantly lower than 100%<sup>10</sup> where most of the discrepancy was attributed to one-prong  $\tau$  decays. During the last year, many new measurements have been performed resulting in a much less significant deficit. However, with the increased precision of the measurements on  $\tau$  lifetime and  $\tau$  decay branching ratios, more fundamental questions can be asked. One of these is the question whether the  $\tau$  is a sequential lepton or not, thus asking whether lepton universality is conserved. Assuming all leptons to be sequential, the leptonic branching fractions of the  $\tau$  lepton can be related to  $\tau$  and  $\mu$  lifetime and masses. In Fig. 1 the Feynman diagram for a generic leptonic decay is shown, where  $l_1$  stands for the decaying leptons  $\mu$  or  $\tau$  and  $l_2$  is  $\mu$  or  $e$  for  $l_1 = \tau$  and  $e$  for  $l_1 = \mu$ . To each vertex,

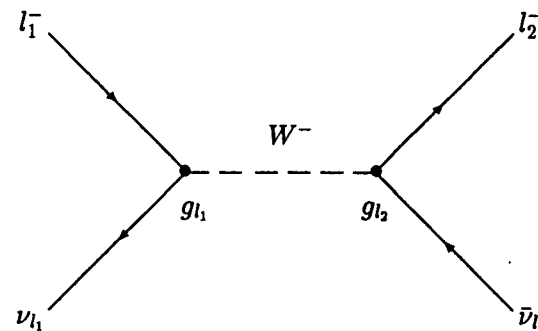


Figure 1: The Feynman-diagram for a leptonic decay  $l_1^- \rightarrow l_2^- \bar{\nu}_{l_2} \nu_{l_1}$ .

a coupling constant can be assigned,  $g_{l_1}$  and  $g_{l_2}$ . Lepton universality requires the coupling constants for all leptons to be equal:  $g_\tau = g_\mu = g_e$ . The Fermi coupling

constant  $G_F$  can be expressed in terms of these coupling constants:

$$G_F^2 = \frac{2g_1^2 g_2^2}{m_W^4}.$$

Thus, the partial decay width for a leptonic decay can be written as:

$$\Gamma(l_1^- \rightarrow l_2^- \bar{\nu}_l \nu_l) = \frac{g_1^2 g_2^2 m_{l_1}^5}{96\pi^3 m_W^4} \cdot f\left(\frac{m_{l_1}^5}{m_{l_2}^5}\right) \cdot (1 + r)$$

where  $r \approx -0.4\%$  arises from radiative corrections and the non-local structure of the  $W$ -propagator<sup>11</sup> and  $f(x)$  is a phase space factor accounting for the mass of  $l_2$ :

$$f(x) = 1 - 8x + 8x^3 - x^4 - 12x^2 \ln x;$$

$f(x)$  equals 1 for  $l_2 = e$  and 0.9728 for  $l_2 = \mu$ . The total decay width is known by a measurement of the lifetime. Lacking other major decay mode but  $\mu^- \rightarrow e^- \bar{\nu}_e \nu_\mu$  for the  $\mu$ ,<sup>12</sup> the total width is then:  $\Gamma(\mu^- \rightarrow e^- \bar{\nu}_e \nu_\mu) = \frac{1}{\tau_\mu}$ , whereas the branching fractions  $B_e$  and  $B_\mu$  have to be considered when calculating the total decay width of the  $\tau$  lepton:

$$\Gamma(\tau^- \rightarrow e^- \bar{\nu}_e \nu_\tau) = \frac{B_e}{\tau_\tau} \quad \text{and} \quad \Gamma(\tau^- \rightarrow \mu^- \bar{\nu}_\mu \nu_\tau) = \frac{B_\mu}{\tau_\tau}.$$

Hence, ratios of coupling constants can be related to the measurable quantities  $B_e$ ,  $B_\mu$ ,  $\tau_\tau$ ,  $\tau_\mu$ ,  $m_\tau$  and  $m_\mu$ :

$$\frac{g_\tau^2}{g_\mu^2} = \left(\frac{m_\mu}{m_\tau}\right)^5 \cdot \frac{\tau_\mu}{\tau_\tau} \cdot B_e$$

and

$$\frac{g_\mu^2}{g_e^2} = \frac{B_\mu}{0.9728 B_e}.$$

Mass and lifetime of the  $\mu$  are known with a very high precision.<sup>12</sup> By the beginning of 1992 the world averages for  $B_e$ ,  $B_\mu$ ,  $\tau_\tau$  and  $m_\tau$  were<sup>12</sup>:  $B_e = (17.93 \pm 0.26)\%$ ,  $B_\mu = (17.58 \pm 0.27)\%$ ,  $\tau_\tau = (305 \pm 6)$  fs and  $m_\tau = (1784.1_{-3.6}^{+2.7})$  MeV/c<sup>2</sup>, implying

$$\frac{g_\mu}{g_e} = 1.004 \pm 0.011$$

and

$$\frac{g_\tau}{g_\mu} = 0.970 \pm 0.013.$$

The  $g_\mu/g_e$  ratio agrees well with the Standard Model expectation of  $g_\mu = g_e$ . It can be compared with the more precise result obtained from leptonic pion decays of  $g_\mu/g_e = 1.0030 \pm 0.0023$ .<sup>13</sup> However, the  $g_\tau/g_\mu$  ratio shows a 2.2 standard

deviation from  $\tau$  and  $\mu$  being sequential leptons. This discrepancy is commonly referred to as the " $\tau$  lifetime problem."<sup>14</sup> If the problem persists it might be the first indication of a violation of lepton universality for the  $\tau$  lepton. In order to prove or disprove an evidence for the violation of lepton universality more and precise measurements of  $B_e$ ,  $B_\mu$ ,  $\tau_\tau$  and  $m_\tau$  are needed. The  $\tau$  mass is of particular interest because the uncertainty of the  $\tau$  mass influences the  $\nu_\tau$  mass measurements: the most sensitive bounds on the mass of the  $\nu_\tau$  can be derived from the analysis of the invariant mass spectrum of semihadronic  $\tau$  decays, e.g., the present best limit of  $m_{\nu_\tau} < 35$  MeV/c<sup>2</sup> (95% CL)<sup>15</sup> was obtained using the decay  $\tau^- \rightarrow \pi^- \pi^- \pi^- \pi^+ \pi^+ \nu_\tau$ . Since this method depends on a determination of the kinematic end point of the mass spectrum, the current precision of the  $\tau$  mass measurement will restrict the ultimate sensitivity on  $m_{\nu_\tau}$  to about 10 MeV/c<sup>2</sup>.

#### The pseudomass $m_\tau^*$

To date, the only method which has been applied in determining the mass of the  $\tau$  lepton is based on the behaviour of the total cross section  $\sigma(e^+e^- \rightarrow \tau^+\tau^-)$  in the threshold region. The four existing measurements lead to an average value of  $m_\tau = (1784.1_{-3.6}^{+2.7})$  MeV/c<sup>2</sup>.<sup>12</sup> However, the result is dominated by the measurement of the DELCO experiment,  $m_\tau = (1782_{-7}^{+2})$  MeV/c<sup>2</sup>,<sup>16</sup> which was later refined to  $m_\tau = (1784.1_{-3.6}^{+2.7})$  MeV/c<sup>2</sup>; after recalibration of the SPEAR energy scale<sup>12</sup> using a high precision  $\psi(2S)$  mass measurement.<sup>17</sup>

In this article I report on a measurement of the  $\tau$  mass using a newly developed pseudomass technique. The  $\tau$  pseudomass is derived from the measured mass, energy and momentum of the three- $\pi$  system in the decay  $\tau^- \rightarrow \pi^- \pi^- \pi^+ \nu_\tau$ , together with the beam energy.

The  $\tau$  mass itself cannot be calculated from the measured quantities since the  $\tau$  flight direction is unknown. However, a  $\tau$  pseudomass can be derived with the approximation that the flight direction of the three- $\pi$  system is the flight direction of the  $\tau$ , i.e., setting  $\cos(\vec{p}_\tau, \vec{p}_{3\pi}) = 1$ . With  $m_\tau^2 = E_\tau^2 - p_\tau^2$  and  $E_\tau = \sqrt{s}/2$ , equal the nominal beam energy, it follows that only the  $\tau$  momentum needs to be determined. Using the approximation noted above, a pseudo  $\tau$  momentum,  $p_\tau^* = p_{3\pi} \pm p_{\nu_\tau}$ , can be derived from the momenta of the three- $\pi$  system and the tau neutrino,  $p_{\nu_\tau}$ . The solution  $p_\tau^* = p_{3\pi} - p_{\nu_\tau}$  has been discarded since the case where  $p_\tau < p_{3\pi}$  is true for only  $\approx 2\%$  of the  $\tau$  decays under consideration. In addition, a poor sensitivity to  $m_\tau$  results from an analysis of such events. The energy of the tau neutrino,  $E_{\nu_\tau}$ , is derived from the energy difference between the  $\tau$  and the three- $\pi$  system:  $E_{\nu_\tau} = E_\tau - E_{3\pi}$ . With  $p_{\nu_\tau} = \sqrt{E_{\nu_\tau}^2 - m_{\nu_\tau}^2}$  and  $m_\tau^{*2} = E_\tau^2 - p_\tau^{*2}$  it follows that:

$$m_\tau^{*2} = 2E_\tau E_{3\pi} - 2E_{3\pi}^2 + m_{3\pi}^2 + m_{\nu_\tau}^2 - 2p_{3\pi} \sqrt{(E_\tau - E_{3\pi})^2 - m_{\nu_\tau}^2}.$$

The mass of the tau neutrino is known to be very small:  $m_{\nu_\tau} < 35 \text{ MeV}/c^2$  (95% CL).<sup>15</sup> The scale of its effect on the pseudomass determination is set by comparison with the other terms  $m_{3\pi}^2$  and  $(E_\tau - E_{3\pi})^2$ . Since the three- $\pi$  system is formed by the decay of an  $a_1$  meson,<sup>18</sup>  $m_{3\pi}$  takes values above  $0.9 \text{ GeV}/c^2$ , i.e., large compared to  $35 \text{ MeV}/c^2$ . Due to the restriction of our choice for  $p_\tau^*$  to  $p_{3\pi} + p_{\nu_\tau}$ , the  $a_1$  meson has been emitted opposite to the  $\tau$  direction of flight (as seen from the  $\tau$  rest frame) for events where the approximation  $\cos(\vec{p}_\tau, \vec{p}_{3\pi}) = 1$  holds true. Since almost no events with  $m_{3\pi}$  masses close to the mass of the  $\tau$  lepton (Fig. 2) have been found, the difference between  $\tau$  and three- $\pi$  energies is large for the majority of events with  $m_\tau^* \approx m_\tau$ , so that here too  $(E_\tau - E_{3\pi}) \gg 35 \text{ MeV}$ . Therefore, a finite but small tau neutrino mass has only a marginal influence on the determination of  $m_\tau$  and will be neglected. Hence,  $m_\tau^{*2}$  can be written as:

$$m_\tau^{*2} = 2(E_\tau - E_{3\pi}) \cdot (E_{3\pi} - p_{3\pi}) + m_{3\pi}^2.$$

The systematic error on  $m_\tau$ , imposed by this approximation, will be discussed later in detail. Another source of systematic uncertainty in the determination of  $m_\tau^*$  is the precision by which the beam energy is known. The absolute energy scale of the DORIS II storage ring has been calibrated using the mass measurements of the  $\Upsilon$  resonances<sup>12,19</sup> as reference. The long term stability of the centre-of-mass energy is known from data taking periods on the  $\Upsilon$  resonances. In addition, the resonance energies have been well reproduced after a shutdown period or after a period of data taking in the nearby continuum. Hence, we conclude that the average beam energy is known with a precision of  $\sigma_{E_{\text{beam}}} \simeq 3 \text{ MeV}$ , yielding a shift to  $m_\tau^*$  of  $\delta m_\tau^* \simeq 0.5 \text{ MeV}/c^2$ , as follows from the formula above. Since the influence of two major possible sources of uncertainty on the determination of the  $\tau$  mass, a finite  $\nu_\tau$  mass and a wrong beam energy, are very small, systematic errors of about  $1 \text{ MeV}/c^2$  should be feasible using the pseudomass method.

#### Data selection

Tau-pair events are selected with the following combinations of decay modes:

$$e^+e^- \longrightarrow \tau^+\tau^- \longrightarrow \pi^-\pi^-\pi^+\nu_\tau$$

└─ 1 – prong final states.

The measurement was performed with the ARGUS detector operating at the  $e^+e^-$  storage ring DORIS II. The data sample, corresponding to  $341 \text{ pb}^{-1}$  and containing about 325 000 produced  $\tau$  pair events, was collected at centre-of-mass energies between 9.4 and 10.6 GeV. The four- $\pi$  spectrometer ARGUS, its trigger requirements and particle identification capabilities have been described in detail elsewhere.<sup>20</sup>

The selection is based on a standard 1-versus-3 topology selection requiring no photons on the three-prong side.<sup>21</sup>

A total of 10959 events passed the selection criteria, including a tau-pair background contribution of  $2161 \pm 200$  events which has been determined from a Monte Carlo study based on the KORALB 2.1/TAUOLA 1.5<sup>†</sup> program package.<sup>22</sup> The dominant fraction of this background originates from the decay  $\tau^- \rightarrow \pi^-\pi^-\pi^+\pi^0\nu_\tau$ , where the photons of the  $\pi^0$  escape undetected.

The background from  $e^+e^-$  annihilation into multihadrons is  $360 \pm 80$  events, as determined by a Monte Carlo study<sup>23</sup> using JETSET versions 6.2 and 6.3<sup>24</sup> as generators. Other background sources, such as Bhabha reactions or two-photon processes, contribute at a level of less than 1% each.

#### $m_\tau$ determination

The measured three- $\pi$  invariant mass spectrum is shown in Fig. 2. Note that the background from other  $\tau$  decays has not been subtracted. The spectrum is compared with Monte Carlo predictions for the invariant  $m_{3\pi}$  spectrum from the decays  $\tau^- \rightarrow a_1^-\nu_\tau$  followed by  $a_1^- \rightarrow \rho^0\pi^-$  and  $\rho^0 \rightarrow \pi^+\pi^-$ , and from the background sources. There is good agreement between data and the Monte Carlo simulation. The small number of entries found for  $m_{3\pi} > 1.8 \text{ GeV}/c^2$  demonstrates that the background from non- $\tau$  events is indeed very small.

The observed pseudomass spectrum after these requirements is shown in Fig. 3 together with the normalized distribution for the background. The data exhibit a sharp threshold behaviour in the region close to the nominal value of the  $\tau$  mass, while the background has only a very slight slope in the same area. The tail above the nominal  $\tau$  mass cannot be explained by the presence of background, but is due to initial-state radiation processes which effectively reduce the  $\tau$  energy. Since the beam energy is used in the calculation of the pseudomass, the true  $\tau$  energy is overestimated, leading to higher values of  $m_\tau^*$ . The position of the pseudomass threshold is directly related to the mass of the  $\tau$  lepton. In Fig. 4 the measured  $m_\tau^*$  spectrum is compared to the Monte Carlo prediction including background. In the simulation of the  $m_\tau^*$  spectrum from  $\tau$  decays, the nominal  $\tau$  mass of  $m_\tau = 1784.1 \text{ MeV}/c^2$  was used. The tail to pseudomasses above the nominal  $\tau$  mass is well reproduced by the Monte Carlo calculation. However, the threshold for the data sample appears to lie below the Monte Carlo expectation for  $m_\tau = 1.7841 \text{ GeV}/c^2$  (enlarged section of Fig. 4), indicating that the  $\tau$  mass is smaller than previously measured.

The shape of the  $m_\tau^*$  spectrum for background has been also determined from the data by an analysis of events which passed the same selection criteria

<sup>†</sup>All Monte Carlo studies on  $\tau$  decays described in this article are based on this program package.

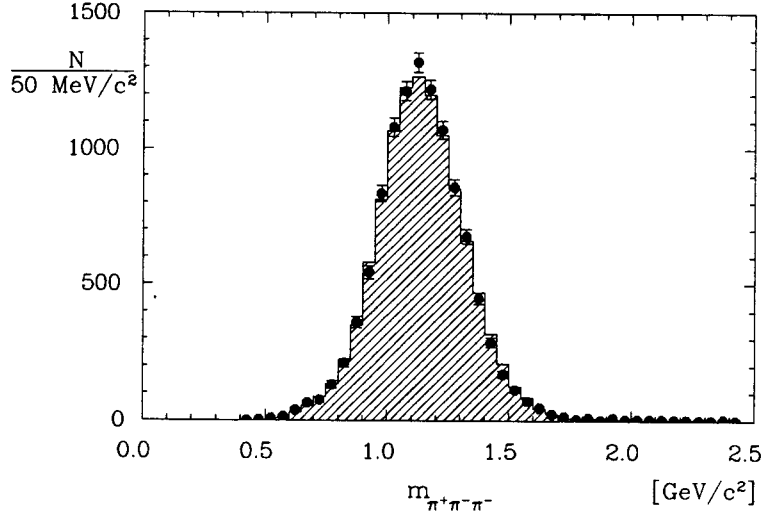


Figure 2: Measured invariant three- $\pi$  mass spectrum. The hatched histogram shows the result of a Monte Carlo calculation of the  $m_{3\pi}$  spectrum for  $\tau$  decays into  $\pi^-\pi^-\pi^+\nu_\tau$  and for background (see text), normalized to the data.

with the exception that two photons were required on the three-prong side. This two-photon system was required to have an invariant mass within  $\pm 100$  MeV/ $c^2$  of the nominal  $\pi^0$  mass<sup>12</sup> and to yield a  $\chi^2 < 9$  when kinematically constrained to the  $\pi^0$  mass. The overall shape of the  $m_\tau^*$  spectrum agrees well with the corresponding spectrum for simulated background events, but shows an even smoother slope in the region close to the nominal mass of the  $\tau$  lepton.

The  $\tau$  mass has been obtained by fitting the measured  $m_\tau^*$  spectrum using a Monte Carlo calculation to determine the expected shape for arbitrary  $\tau$  masses. Monte Carlo studies have shown that the  $m_\tau^*$  spectrum for different  $m_\tau$  masses can be obtained by a simple shift of the spectrum with respect to a simulated  $m_\tau^*$  spectrum for a reference  $\tau$  mass  $m_\tau^0$  (here  $m_\tau^0 = 1.7841$  GeV/ $c^2$ ), provided the  $\tau$ -mass difference  $\delta m_\tau$  to  $m_\tau^0$  is small:

$$f(m_\tau^*, m_\tau = m_\tau^0 + \delta m_\tau) = f(m_\tau^* - \delta m_\tau, m_\tau = m_\tau^0)$$

where  $f(m_\tau^*, m_\tau^0)$  describes the expected shape of a  $m_\tau^*$  spectrum for the reference  $\tau$  mass. The simulated  $m_\tau^*$  spectrum for  $\tau$  decays into  $\tau^- \rightarrow \pi^-\pi^-\pi^+\nu_\tau$  is shown in Fig. 5. Note that the influence of the beam energy spread of the DORIS II

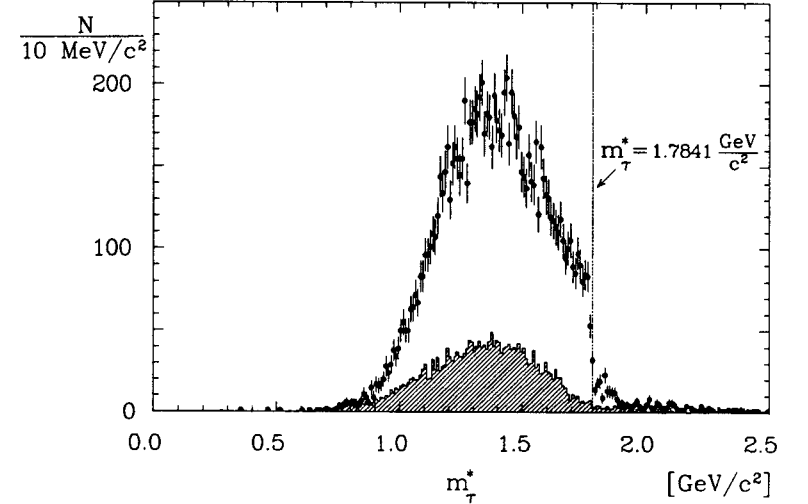


Figure 3: Tau pseudomass spectrum of data (full dots with error bars) and background, normalized to the data (hatched histogram). The present nominal  $\tau$  mass of  $m_\tau^* = m_\tau = 1.7841$  GeV/ $c^2$ <sup>12</sup> is indicated by the dotted line.

storage ring is included in the simulation. The shape of the spectrum has been modelled in the region  $1.65$  GeV/ $c^2 < m_\tau^* < 1.9$  GeV/ $c^2$  with a heuristic function of the form:

$$f(m_\tau^*, m_\tau^0) \sim a_1 \left( \frac{1}{e^{a_4 \cdot \frac{m_\tau^* - a_3}{1 - a_5 \cdot m_\tau^*}} + 1} \cdot (1 + a_2 \cdot m_\tau^*) \right)$$

where  $a_i$  with  $i = 1..5$  are free parameters.

In the fit to the data we used the same function with all parameters fixed to the values extracted from the simulation except the normalization  $a_1$ . The data have been fitted in the region  $1.7$  GeV/ $c^2 < m_\tau^* < 1.85$  GeV/ $c^2$ , limiting possible shifts in the  $\tau$  mass to  $\delta m_\tau < 50$  MeV/ $c^2$ . Although the background is small in this region and does not exhibit any threshold behaviour, we have included its contribution in the fit. The background  $m_\tau^*$  spectra from  $\tau$  decays and multihadron sources have been parametrized, leaving only the overall normalization as a free parameter. Hence, the fit to the observed  $m_\tau^*$  spectrum has four free parameters:  $m_\tau$  and the normalizations for the three contributing functions. By this procedure we

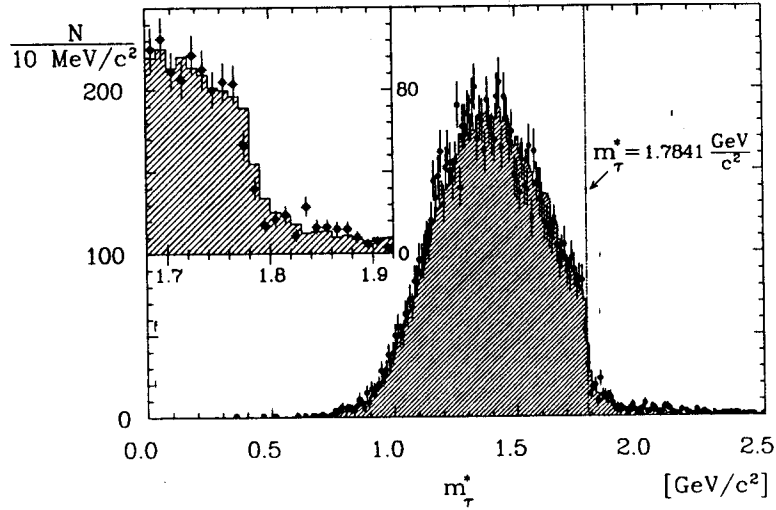


Figure 4: Measured three- $\pi$  pseudomass spectrum compared with the result from a Monte Carlo calculation (hatched histogram) of the  $m_\tau^*$  spectrum for  $\tau$  decays into  $\pi^-\pi^-\pi^+\nu_\tau$  and for background, normalized to the data. The present nominal  $\tau$  mass of  $m_\tau^* = m_\tau = 1.7841 \text{ GeV}/c^2$ <sup>12</sup> is indicated by the dotted line. The enlarged section in the upper left-hand corner provides a detailed view of the pseudomass region  $1.68 \text{ GeV}/c^2 \leq m_\tau^* \leq 1.92 \text{ GeV}/c^2$ .

obtain a  $\tau$  mass of:

$$m_\tau = (1776.3 \pm 2.4) \text{ MeV}/c^2$$

where only the statistical error is given. The measured  $m_\tau^*$  spectrum is shown in Fig. 6 together with the fitted function. The threshold, visible in the data, and the expected background level, are well reproduced by the fit.

In order to determine the systematic error a variety of sources have been considered. A  $\nu_\tau$  mass of  $m_{\nu_\tau} = 20 \text{ MeV}/c^2$  would cause a shift in  $m_\tau$  of  $\delta m_\tau \approx 0.3 \text{ MeV}/c^2$ . A systematic deviation of the beam energy from its nominal value by 3 MeV results in a change of  $\delta m_\tau = 0.5 \text{ MeV}/c^2$ . Within statistical errors the obtained result did not change by analyzing the  $m_\tau^*$  spectra for arbitrary subsets of the data sample, thereby accounting for different centre-of-mass energies at which the data have been taken. The absolute momentum scale of the experiment is known to  $\pm 0.15\%$ ,<sup>25</sup> as determined from reconstructed  $K_S^0$  mesons in

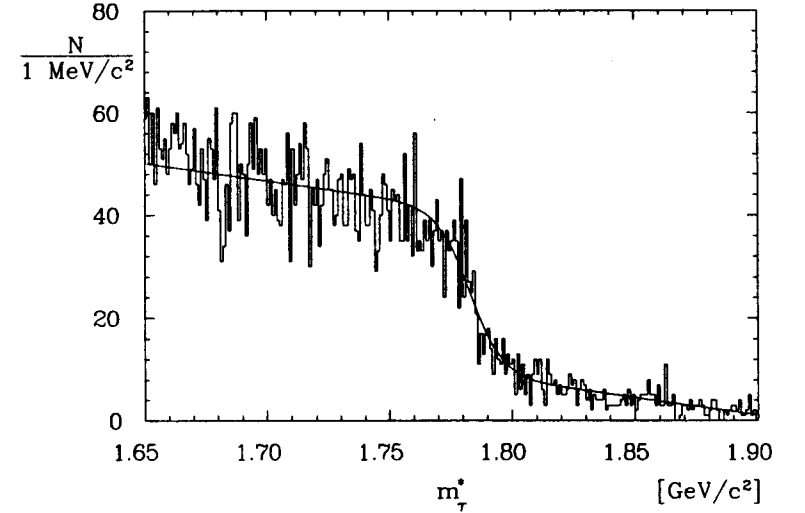


Figure 5: Simulated pseudomass spectrum for  $\tau$  decays of the type  $\tau^- \rightarrow \pi^-\pi^-\pi^+\nu_\tau$  ( $m_\tau = 1784.1 \text{ MeV}/c^2$ ). The curve shows the result of the fit described in the text.

various momentum and angular intervals, leading to  $\delta m_\tau = 1.2 \text{ MeV}/c^2$ . The fit procedure has been checked by varying the fit region, allowing for different background contributions, using different parametrizations to model the simulated  $m_\tau^*$  spectrum and accounting for possible deviations between the measured and simulated three- $\pi$  mass spectra. The latter test has been performed since the shape of the threshold behaviour visible in the  $m_\tau^*$  spectrum depends slightly on the three- $\pi$  mass.<sup>§</sup> The extracted  $m_\tau$  values were stable at a level of  $\delta m_\tau = 0.5 \text{ MeV}/c^2$ .

From these considerations, the systematic error on the fitted  $\tau$  mass is determined to be  $\sigma_{sys}(m_\tau) = 1.4 \text{ MeV}/c^2$  by adding each individual error quadratically, leading to a final tau mass result of:

$$m_\tau = (1776.3 \pm 2.4 \pm 1.4) \text{ MeV}/c^2.$$

Adding statistical and systematic errors in quadrature yields a total error of  $\sigma_{tot}(m_\tau) = 2.8 \text{ MeV}/c^2$ , which is comparable to the error of the present world average  $\sigma_{PDG}(m_\tau) = {}^{+2.7}_{-3.6} \text{ MeV}/c^2$ .<sup>12</sup> The central value of our measurement is

<sup>§</sup>The determination of  $m_\tau$  does not rely on events where  $m_{3\pi} \approx m_\tau$ .

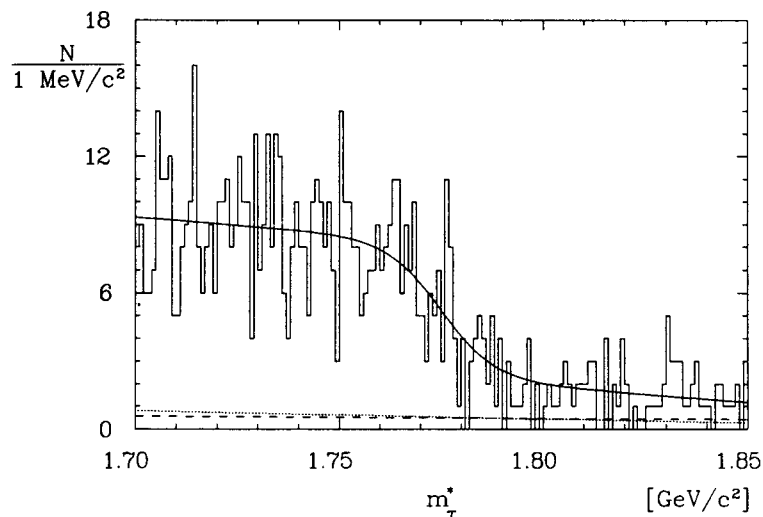


Figure 6: Measured  $m_{\tau}^*$  spectrum in the region of the threshold close to the  $\tau$  mass. The curves show the results of the fit described in the text (broken line: fitted background) and the expected background level (dotted line).

smaller than the world average by  $7.8 \text{ MeV}/c^2$ , a discrepancy of about 1.7 standard deviations. No attempt has been made to calculate a new world average using our measurement since all previous measurements are based on a different method, the determination of the cross section  $\sigma_{\tau\tau} = \sigma(e^+e^- \rightarrow \tau^+\tau^-)$  close to the production threshold.

The measurement of the  $\tau$  mass presented here gives first evidence that the  $\tau$  mass is significantly lower than has been previously inferred. Using our measured  $\tau$  mass for the calculation of the  $g_{\tau}/g_{\mu}$  ratio yields:  $g_{\tau}/g_{\mu} = 0.981 \pm 0.013$ . Thus, evidence for a possible violation of the lepton universality becomes weaker and appears now to have a significance of 1.5 standard deviations.

#### A new upper limit on the $\nu_{\tau}$ mass

The downward shift in the  $\tau$  mass by  $\delta m_{\tau} = 7.8 \text{ MeV}/c^2$  also affects the upper limit on the mass of the  $\tau$  neutrino. In 1987 we reported an improved upper limit on the  $\nu_{\tau}$ -mass of  $m_{\nu_{\tau}} < 35 \text{ MeV}/c^2$  at 95% confidence level.<sup>15</sup> The limit had been obtained from an analysis of the invariant five- $\pi$  mass spectrum of the decay  $\tau^- \rightarrow \pi^- \pi^- \pi^- \pi^+ \pi^+ \nu_{\tau}$ . Since 1987 the available data sample has been enlarged,

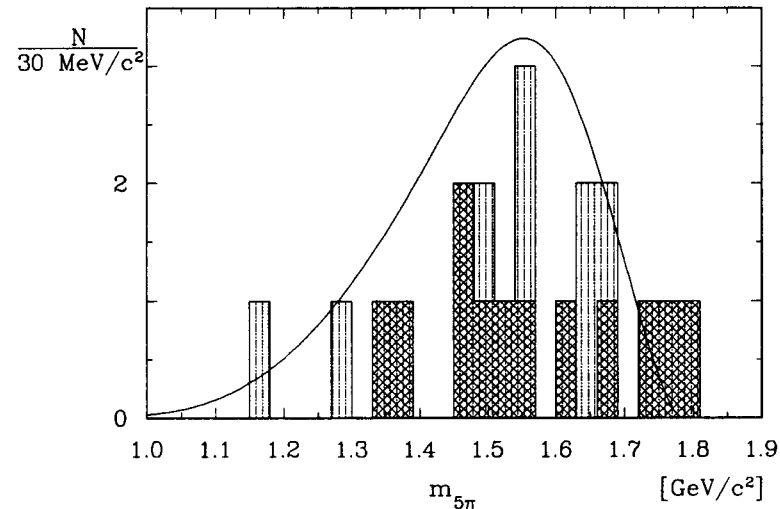


Figure 7: Measured invariant five- $\pi$  mass spectrum (histogram), where the hatched part displays the result of our previous analysis (see text). The curve corresponds to the expected shape of a phase-space decay weighted with the weak matrix element (assuming  $m_{\nu_{\tau}} = 0 \text{ MeV}/c^2$ ). Note that the curve has not been normalized to the data.

corresponding now to an integrated luminosity of  $387 \text{ pb}^{-1}$  compared to  $197 \text{ pb}^{-1}$  in 1987. In order to gain more information about the mass of the  $\nu_{\tau}$ , the analysis has been repeated. Including the old data, 20 (12)<sup>¶</sup> events are now selected, from which 19 (11) were used to determine the upper limit on the mass of the  $\nu_{\tau}$ . As discussed in our previous publication<sup>15</sup> the event with the highest five- $\pi$  mass has been removed in order to account for possible uncertainties in the background determination.

The invariant mass spectrum of the 20 events is shown in Fig. 7. Also shown in this figure is the expectation for a phase-space decay weighted by the weak matrix element, which is in reasonable agreement with the data. In addition, it can be seen that for the new data sample no event with a five- $\pi$  mass close to the end point has been recorded. Therefore, the analysis of the five- $\pi$  mass spectrum yields no change of the limit on the  $\nu_{\tau}$ , despite the increase of data sample's size; it remains at  $m_{\nu_{\tau}} < 35 \text{ MeV}/c^2$  (95% CL), assuming a  $\tau$  mass of  $1.7841 \text{ GeV}/c^2$ . Using the

<sup>¶</sup>The numbers in parentheses correspond to the analysis of 1987.

$\tau$  mass obtained in this analysis as the end point of the five- $\pi$  mass spectrum the revised upper limit on  $m_{\nu_\tau}$  is determined to be:

$$m_{\nu_\tau} < 31 \text{ MeV}/c^2,$$

at the 95% confidence level.

#### Measurement of the decay $\tau^- \rightarrow \rho^- \nu_\tau$

Although the so-called  $\tau$ -decay problem, i.e., the discrepancy between the measured exclusive and inclusive  $\tau$  branching ratios, became less significant during the past year, it is still highly desirable to determine exclusive branching ratios as independent as possible from other measurements: All  $\tau$  branching ratios have been measured at  $e^+e^-$  colliders where  $\tau$  leptons are produced in pairs, this correlation might influence the measurement of an exclusive branching ratio when other  $\tau$ -decays are used as reference. An almost independent determination can be achieved for the major decay modes by selecting  $\tau$ -pair events where both  $\tau$ 's decay into the same final state. Unfortunately most of the existing data samples have not been large enough to allow a precise determination of  $\tau$  branching ratios using this procedure.

ARGUS performed the first measurement of tau-pair decays into  $\pi^\pm \pi^0 \nu_\tau$ , allowing a determination of the branching ratio  $\text{Br}(\tau^- \rightarrow \pi^- \pi^0 \nu_\tau)$  without using a topological or any other exclusive decay mode as reference. The decay  $\tau^- \rightarrow \pi^- \pi^0 \nu_\tau$  is favourable for such measurements since it has the largest single-prong branching ratio of  $(23.01 \pm 0.55)\%$ .<sup>26</sup> The channel  $\tau^- \rightarrow \pi^- \pi^0 \nu_\tau$  is known to be dominated by the decay  $\tau^- \rightarrow \rho^- \nu_\tau$ ; only one measurement of nonresonant  $\pi^- \pi^0$  production has been reported so far, with a branching ratio of  $(0.3 \pm 0.1 \pm 0.3)\%$ .<sup>12</sup>

The invariant  $\pi^- \pi^0$  mass spectrum can be related to the data for the isospin  $I = 1$  part of the cross section for the process  $e^+e^- \rightarrow \pi^+ \pi^-$  by means of the conserved vector current (CVC) hypothesis. The  $e^+e^-$  data show that the spectrum cannot be described entirely by the presence of the  $\rho$  resonance.<sup>27</sup> CVC requires these deviations to be visible in the  $\tau$  data also.

In addition, a test of the structure of the interaction in the decay  $\tau^- \rightarrow \rho^- \nu_\tau$  can be performed. The nature of the weak interaction implies the presence of a vector-like coupling. Regardless of the admixture of vector and axial-vector couplings, a vector-like coupling requires both fermions at one vertex to prefer the same handedness, which imposes constraints on the population density of different  $\rho$  helicity states.<sup>†</sup> The angular distribution of the pions in the  $\rho$  rest frame with respect to the  $\rho$  direction of flight is a sensitive measure of this aspect of the coupling. Note that this method cannot distinguish between the helicity

<sup>†</sup>In this paper the measured  $\pi^- \pi^0$  system will often be called " $\rho$ " for simplicity.

$H_\rho = 1$  and  $H_\rho = -1$ , but can show the relative population of states with  $H_\rho = 0$  or  $|H_\rho| = 1$ .

The polarization of  $\tau$  leptons produced in  $Z^0$  decays can be measured using several  $\tau$  decay channels, where the highest sensitivity has been achieved for the decay  $\tau^- \rightarrow \rho^- \nu_\tau$ .<sup>28</sup> However, this analysis relies on a spin alignment of the  $\rho$  which is predicted by the Standard Model but has not been tested experimentally with high precision up to now.

The population density of the allowed  $\rho$  helicity states is also sensitive to the spin of the  $\tau$ -neutrino. Under the assumption that the  $\nu_\tau$  is massless only the spins  $J_{\nu_\tau} = \frac{1}{2}$  and  $J_{\nu_\tau} = \frac{3}{2}$  are allowed. It can be shown that the two  $\nu_\tau$  spin hypotheses yield different decay angular distributions for the pions.

The analysis of the decay  $\tau^- \rightarrow \rho^- \nu_\tau$  presented here comprises three parts: (a) determination of the branching ratio  $\text{Br}(\tau^- \rightarrow \pi^- \pi^0 \nu_\tau)$ , analysis of (b) the invariant  $\pi^- \pi^0$  mass spectrum and (c) the spin alignment of the  $\rho$ .

#### Data selection

The event sample used for this analysis corresponds to an integrated luminosity of  $264 \text{ pb}^{-1}$ , with about 262 000 produced  $\tau$  pairs. One major objective of this analysis is to determine the branching ratio  $\text{Br}(\tau^- \rightarrow \pi^- \pi^0 \nu_\tau)$  as independently as possible of other measurements. This was achieved by selecting  $\tau$  pair events with both  $\tau$ 's decaying into  $\pi^\pm \pi^0 \nu_\tau$ :

$$e^+e^- \longrightarrow \tau^+\tau^- \longrightarrow \pi^- \pi^0 \nu_\tau$$

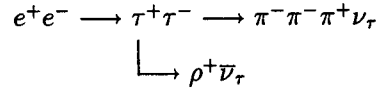
└───  $\pi^+ \pi^0 \nu_\tau$

In this case, the branching ratios for other  $\tau$  decays enter only in the calculation of the background. The only major background source is from other  $\tau$  decays, while contamination from non- $\tau^+\tau^-$  events is reduced to a negligible level by the selection procedure. Such events have been extracted from a special two-prong data sample containing 3 947 617 events. This initial data set was obtained by applying only moderate cuts which mainly reject Bhabha events. Monte Carlo studies have shown that the total selection efficiency is decreased by only  $(1.7 \pm 0.3)\%$  due to these requirements. Energy clusters in the calorimeter of more than 80 MeV with no associated track are accepted as photon candidates. The number of photons per event is restricted to be 2, 3 or 4. Although four photons are produced in the events by the decay of the  $\pi^0$ 's, a smaller number may be measured, even if no photon escapes detection, because photons from a high energy  $\pi^0$  often merge into one single cluster in the electromagnetic calorimeter. In order to account for this effect, for each  $\pi^\pm \pi^0$  candidate either one or two photons are allowed. If only one photon is found in a given hemisphere it must have at least an energy of 1 GeV



to be compatible with being a merged cluster, otherwise the event is rejected. This photon is treated as a  $\pi^0$  for further analysis. The two-photon system of one hemisphere must have an invariant mass within  $\pm 100 \text{ MeV}/c^2$  of the nominal  $\pi^0$  mass<sup>12</sup> and yield a  $\chi^2 < 9$  when kinematically constrained to the  $\pi^0$  mass. The selection requirements are satisfied by 1249 events, which are then used to determine the branching ratio for  $\tau^- \rightarrow \pi^- \pi^0 \nu_\tau$ .

For the study of the  $\pi^- \pi^0$  invariant mass spectrum and the decay angular distribution, the data sample was augmented by an additional selection of events where one of the  $\tau$ 's was allowed to decay into three charged pions:



The requirements for the  $\pi^- \pi^0$  system have been kept identical to those for the 1-versus-1 prong sample. This procedure guarantees that the shape of the  $\pi^- \pi^0$  mass spectra in both data samples will be equal after subtraction of the background from non- $\tau$  events. The selection of these events is based on a standard 1-versus-3 topology with the cuts adjusted to the specific decay mode.<sup>29</sup> The selection requirements are satisfied by 1772 events. Although the backgrounds from  $\tau$  pair events differ in the two decay topologies, the fractional contributions from this source are the same in both  $\pi^- \pi^0$  mass spectra. This behaviour is expected since background to the three- $\pi$  decay does not influence the decay of the other tau.

#### Branching ratio for the decay $\tau^- \rightarrow \pi^- \pi^0 \nu_\tau$

The background from non- $\tau$  pair reactions in events with the 1-versus-1 topology is found to be very small. The selection requirements reject background from  $\Upsilon$  resonance decays entirely, as verified by Monte Carlo studies. The method for finding the number of hadronic background events is based on Monte Carlo generation of  $q\bar{q}$  events including initial-state radiation (JETSET version 6.2 and 6.3<sup>24</sup>). Only 13 out of a generated sample of 783 000 events pass all selection criteria. The reconstructed  $\pi^- \pi^0$  masses of these events are inside the  $\rho$  mass region. The background level in the data has been determined to be  $15 \pm 4$  events by scaling this result to the integrated luminosity of the data. Two photon reactions have also been considered. Here, the process  $\gamma\gamma \rightarrow \pi^+\pi^-\pi^0\pi^0$  deserves particular attention, since a major fraction of the final state is produced as a  $\rho\rho$  system.<sup>30</sup> However, Monte Carlo studies have shown the background from two-photon reactions is only  $9 \pm 5$  events. The selection criteria have been specifically designed to exclude a large contribution from Bhabha events. The residual background is determined by a study of the selected data sample in phase space regions which are preferably populated by such events. The small number of events found here

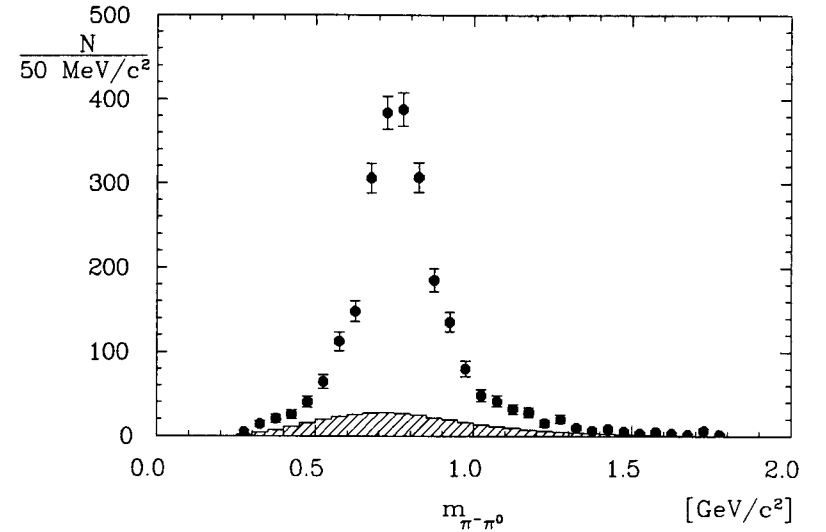


Figure 8: Invariant  $\pi^- \pi^0$  mass spectrum after the subtraction of the background from non- $\tau$  pair events. Note that there are two entries per event. The hatched histogram shows the mass spectrum for background from  $\tau$  pair events.

leads to a conservative estimate of  $8 \pm 4$  events from Bhabha sources. The total background from non- $\tau^+\tau^-$  events is thus  $32 \pm 7$ . The invariant  $\pi^- \pi^0$  mass spectrum after subtraction of the non- $\tau^+\tau^-$  background is shown in Fig. 8 together with the expectation of the background from  $\tau$  pair events. The mass spectrum exhibits a clear  $\rho$  signal.

The background from  $\tau^+\tau^-$  events can be divided into two classes: (1) events in which neither  $\tau$  decays into  $\pi^- \pi^0 \nu_\tau$ , and (2) events in which only one  $\tau$  decays into  $\pi^- \pi^0 \nu_\tau$ . To determine the efficiency for selecting the signal events and level of any background from  $\tau$  decays, extensive Monte Carlo simulations have been performed. In our calculations, the branching ratios for 'background' decays were taken from Refs. 26 and 31. If neither tau decays into  $\pi^- \pi^0 \nu_\tau$  (class 1), the background is determined to be  $33.6 \pm 7.1$  events. If one tau decays into  $\pi^- \pi^0 \nu_\tau$  (class 2), the background cannot be calculated without knowing the branching ratio for  $\tau^- \rightarrow \pi^- \pi^0 \nu_\tau$ . Rather than using an iterative procedure starting from the current world average value of  $(23.01 \pm 0.55)\%$  for this branching ratio, we

have chosen instead to solve the following equation for  $Br_1$ :

$$N_{\tau\tau} \cdot (\epsilon_{11} Br_1^2 + 2 \cdot Br_1 \cdot \Sigma(\epsilon_{1i} Br_i)) = N_{\text{corr}},$$

where  $Br_1$  denotes  $Br(\tau^- \rightarrow \pi^- \pi^0 \nu_\tau)$ ,  $Br_i$  is the branching ratio of a 'background'  $\tau$  decay (note that all decay channels leading to one or three charged particles in the final state have been taken into account),  $N_{\text{corr}} = 1183.4 \pm 10.0$  is the number of selected events after subtraction of background from non- $\tau^+\tau^-$  events and from  $\tau^+\tau^-$  events with no  $\tau$  decaying into  $\pi^- \pi^0 \nu_\tau$ ,  $N_{\tau\tau} = 261500 \pm 5420$  is the number of  $\tau$  pairs produced,  $\epsilon_{11}$  is the efficiency for selecting a  $\tau^+\tau^-$  event where both  $\tau$ 's decays into  $\pi^\pm \pi^0$ , and  $\epsilon_{1i}$  is the efficiency for selecting events where one tau decays into  $\pi^- \pi^0 \nu_\tau$  while the other decays into the 'background' channel  $i$ . The efficiency calculation includes the influence of the trigger, as well as the effect of fake photons produced by noise in the electromagnetic calorimeter and by split-offs from the shower cluster associated with the charged particle.<sup>32</sup> The trigger simulation has been developed and extensively checked from the data itself; systematic errors include the effects of any residual deviations. Likewise the simulation of the probability for a fake photon has been confirmed with cosmic ray data. The efficiency  $\epsilon_{11}$  has been determined to be  $(6.68 \pm 0.24)\%$ . From this we calculate a value for the branching ratio of:

$$Br(\tau^- \rightarrow \pi^- \pi^0 \nu_\tau) = (22.6 \pm 0.4 \pm 0.9)\%.$$

The probability that one  $\pi^- \pi^0$  system is produced by a 'background' decay is  $(14.9 \pm 1.7)\%$ . The background from  $\tau$  pair events, where one  $\tau$  decays into  $\pi^- \pi^0 \nu_\tau$  is  $295 \pm 40$  events. The largest fraction ( $\approx 60\%$ ) from this source is due to the decay  $\tau^- \rightarrow \pi^- \pi^0 \pi^0 \nu_\tau$ , with a branching ratio of  $(7.9 \pm 0.5)\%$ .<sup>33</sup> Since this hadronic final state originates from the decay  $a_1^- \rightarrow \rho^- \pi^0$ ,<sup>18</sup> the invariant  $\pi^- \pi^0$  mass spectrum contains a  $\rho$  signal due to a lost  $\pi^0$  from the direct  $a_1^-$  decay. The other major source is due to the decay chain  $\tau^- \rightarrow K^{*-} \nu_\tau$ , with a branching ratio of  $(1.45 \pm 0.13)\%$ ,<sup>28</sup> followed by  $K^{*-} \rightarrow K^- \pi^0$ . Here, the lack of a particle identification requirement does not allow one to distinguish the two channels.

#### Analysis of the $\pi^- \pi^0$ mass spectrum

For the analysis of the  $\pi^- \pi^0$  invariant mass spectrum and the spin alignment of the  $\rho$ , both selected data samples were used. The background from non- $\tau$  pair reactions in the 1772 events with the 1-versus-3 topology has been determined by a similar means to that described above for the branching ratio. The contribution is found to be  $155 \pm 41$  events, of which most are due to  $q\bar{q}$  reactions. After subtraction of background from non- $\tau^+\tau^-$  events the mass spectra from both samples have the same shape and equal background contributions from  $\tau$

decays. This feature has been achieved by choosing identical requirements for the reconstruction of the  $\pi^- \pi^0$  system. The invariant  $\pi^- \pi^0$  mass spectrum after subtraction of background from  $\tau^+\tau^-$  events is shown in Fig. 9, and contains 3448  $\rho$ -candidates.

In the framework of CVC, the invariant  $\pi^- \pi^0$  mass spectrum can be described by the following formula<sup>34</sup>:

$$\frac{d\Gamma(q^2)}{dq} = \frac{G_F^2}{16\pi^2 m_\tau^3} q(m_\tau^2 - q^2)^2 (m_\tau^2 + 2q^2) v_1(q^2).$$

where  $v_1(q^2)$  denotes the spectral function and  $q^2$  corresponds to  $m_{\pi^- \pi^0}^2$ . For the decay  $\tau^- \rightarrow \pi^- \pi^0 \nu_\tau$ , the spectral function  $v_1(q^2)$  can be related to the cross section for  $e^+e^-$  annihilation into  $\pi^- \pi^+$  with isospin  $I = 1$ :

$$v_1(q^2) = \frac{q^2 \cdot \sigma_{I=1}^{e^+e^- \rightarrow \pi^+ \pi^-}(q^2)}{4\pi^2 \alpha^2}.$$

The total cross section ( $I = 1, 0$ ) is given by:

$$\sigma_{I=1,0}^{e^+e^- \rightarrow \pi^+ \pi^-} = \frac{\pi \alpha^2}{3q^2} \left(1 - \frac{4m_\pi^2}{q^2}\right)^{\frac{1}{2}} |F_\pi|^2.$$

Recently, Kühn and Santamaria<sup>27</sup> fitted the available data on the pion form factor  $|F_\pi|^2$ , using a variety of parametrizations. The only known  $I = 0$  contribution comes from the decay  $\omega \rightarrow \pi^+ \pi^-$ , leading to so-called  $\rho - \omega$  interference. Thus, the  $|F_\pi^{I=1}|^2$  contribution is obtained by removing this contribution. We use one of the parametrizations<sup>27</sup> to describe  $|F_\pi|^2$ :

$$F_\pi(q^2) = BW_\rho \frac{1 + \alpha BW_\omega}{1 + \alpha} \cdot \begin{cases} \tilde{g}(q^2) & q^2 > (m_\omega + m_\pi)^2 \\ \text{Re}(\tilde{g}(q^2)) & q^2 \leq (m_\omega + m_\pi)^2 \end{cases}$$

with

$$\tilde{g}(q^2) = \left( \frac{m_0^2}{m_0^2 - q^2 - im_0 \Gamma_0} \right)^{n_0}.$$

Here,  $BW$  denotes a relativistic Breit-Wigner as proposed by Gounaris and Sakurai.<sup>35</sup> The factors  $\alpha$  and  $BW_\omega$  are used to describe the  $\rho - \omega$  interference contribution, which is not present in the  $\tau$  case. Hence,  $\alpha$  is set to zero in our analysis. The function  $\tilde{g}$ <sup>36</sup> is used to describe the deviation of  $|F_\pi|^2$  from a pure Breit-Wigner, which is visible in the "high" mass range above  $0.8 \text{ GeV}/c^2$ . This deviation is sometimes interpreted as evidence for radially excited  $\rho$ -mesons.<sup>37</sup> The fit<sup>27</sup> to  $|F_\pi|^2$  yielded the following results:  $m_\rho = 0.776 \text{ GeV}/c^2$ ,  $\Gamma_\rho = 0.149 \text{ GeV}/c^2$ ,  $m_0 = 1.180 \text{ GeV}/c^2$ ,  $\Gamma_0 = 0.105 \text{ GeV}/c^2$  and  $n_0 = 0.142$ . From the integration of  $|F_\pi^{I=1}|^2$  a prediction follows for the ratio of the branching ratios into  $\pi^- \pi^0 \nu_\tau$  and  $e^- \nu_\tau$  of  $Br(\tau^- \rightarrow \pi^- \pi^0 \nu_\tau) / Br(\tau^- \rightarrow e^- \bar{\nu}_e \nu_\tau) = 1.32 \pm 0.05$ .<sup>27</sup>

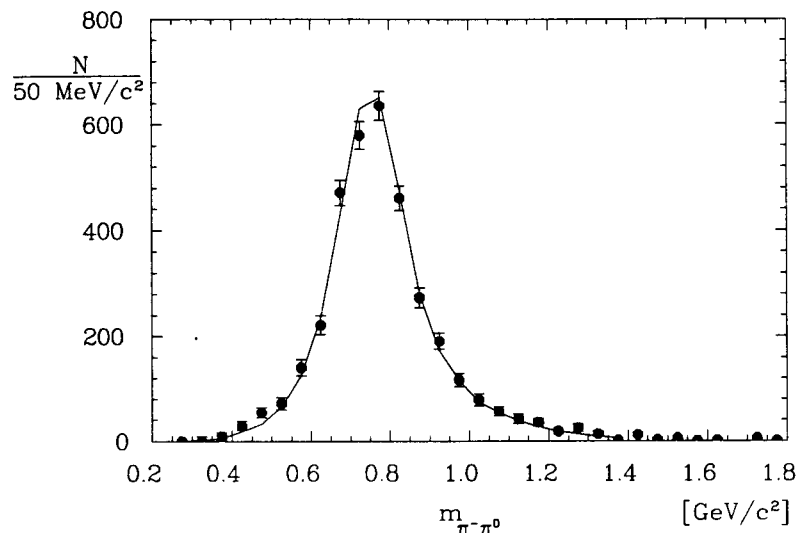
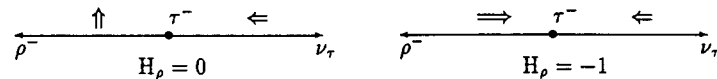


Figure 9: Background subtracted  $m_{\pi^-\pi^0}$  spectrum. The curve shows the CVC prediction, with the detector acceptance applied to it.

When comparing the CVC prediction to the data, acceptance effects, including detector resolution, are accounted for in the model prediction instead of deconvoluting the measured mass spectrum. The fit has been restricted to the region of  $0.28 \leq m_{\pi^-\pi^0} \leq 1.4$   $\text{GeV}/c^2$ , and includes only the normalization as a free parameter. The background corrected  $m_{\pi^-\pi^0}$  spectrum is shown together with the CVC prediction in Fig. 9. The  $\chi^2$  for the fit is 22.5 for 22 degrees of freedom. If the  $\pi^-\pi^0$  mass spectrum is fitted by describing  $|F_\pi|^2$  as a pure  $\rho$  Breit-Wigner,  $BW_\rho$ , the  $\chi^2$  increases to 38.7. We conclude that the entire mass spectrum is in good agreement with the spectral function obtained from the CVC related process  $e^+e^- \rightarrow \pi^+\pi^-$ . This result serves as a further check for our branching ratio measurement, confirming that the acceptance effects are well understood.

#### Measurement of the spin alignment of the $\rho$

The  $\tau$  lepton has been shown to be a spin  $\frac{1}{2}$  particle from measurements of the production cross section  $e^+e^- \rightarrow \tau^+\tau^-$  near threshold.<sup>12</sup> According to the Standard Model the  $\nu_\tau$  must have spin  $\frac{1}{2}$  also. With this assumption the  $\nu_\tau$  has been demonstrated to be left-handed.<sup>9</sup> Therefore, only two helicity states of the  $\rho^-$  are allowed in the decay  $\tau^- \rightarrow \rho^-\nu_\tau$ :



Neglecting mass effects,  $\tau$  and  $\nu_\tau$  have the same handedness due to the vector-like nature of the coupling, thus imposing constraints on the helicity of the  $\rho$ . If both are left-handed, only the helicity state  $H_\rho = 0$  is allowed. Mass effects allow different handedness for the  $\tau$  and  $\nu_\tau$ . The ratio of the probabilities for the  $\tau$  to be right-handed  $R$  and left-handed  $L$  in this coupling is a function of the  $\tau$  velocity  $\beta$  (in the  $\rho$  rest frame):

$$\frac{L}{R} = \frac{1 + \beta}{1 - \beta},$$

where, for the decay  $\tau^- \rightarrow \rho^-\nu_\tau$ :

$$\beta = \frac{m_\tau^2 - m_\rho^2}{m_\tau^2 + m_\rho^2}.$$

In the following calculations the  $\tau$  is assumed to be at rest and 'helicity' of the  $\tau$  is defined with respect to the  $\nu_\tau$  direction of flight. In this case, the figure above shows that the  $\tau$  couples left-handed (as seen from the  $\rho$ ) for the  $\rho$  helicity  $H_\rho = 0$  and right-handed for  $H_\rho = -1$ , respectively. Hence  $H_\rho = 0$  is favoured by  $L/R = m_\tau^2/m_\rho^2$ . The angular distribution of the pions in the  $\rho$  rest frame relative to its direction of flight can be written as:

$$\frac{dN}{d \cos \vartheta} \sim \frac{L}{R} \cos^2 \vartheta + \sin^2 \vartheta,$$

which is equivalent to:

$$\frac{dN}{d \cos \vartheta} \sim 1 + b_\tau \cos^2 \vartheta \quad \text{with} \quad b_\tau = \frac{m_\tau^2 - m_\rho^2}{m_\rho^2}.$$

In the narrow width approximation, where  $\Gamma_\rho$  is neglected, one obtains:  $b_\tau = 4.4$ .

The above considerations can only be exploited if the  $\tau$  is at rest. In the case of a  $\tau$  produced in motion, the direction of flight of the  $\rho$  in the  $\tau$  rest frame is no longer known. However, the angular distribution of the pions in the  $\rho$  rest frame relative to the  $\rho$  direction of flight in the laboratory system still shows a

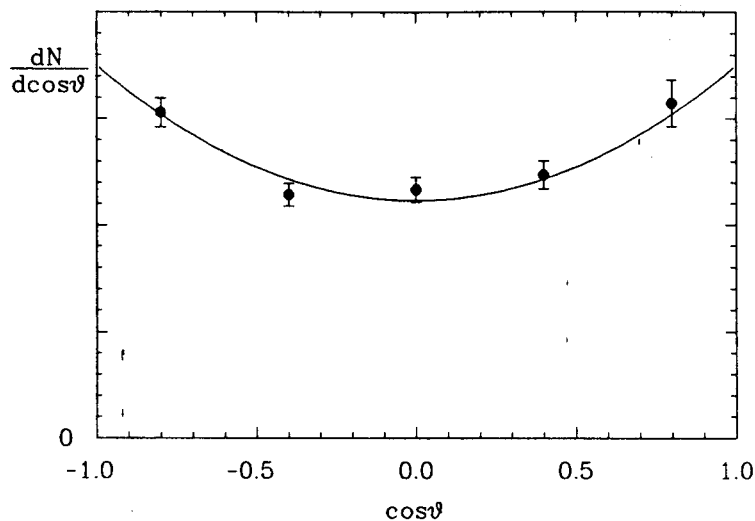


Figure 10: Angular distribution of the pions in the  $\rho$  rest frame with respect to the observed  $\rho$  direction of flight after background subtraction and efficiency correction. The curve shows the result of a fit which is described in the text. The vertical scale is arbitrary.

distribution proportional to  $1 + b \cos^2 \vartheta$ , with  $b \neq b_\tau$ . The parameter  $b$  depends strongly on the velocity of the  $\tau$  lepton in the laboratory frame. Since  $b$  shows almost no variation over the DORIS II energy range, the ARGUS data from all centre-of-mass energies can be combined in the analysis. The parameters  $b_\tau$  and  $b$  are extremely sensitive to the shape of the invariant  $\pi^- \pi^0$  mass spectrum. Since we have shown that the mass spectrum can be well described by means of CVC, the parametrization of Kühn and Santamaria<sup>27</sup> can be used to calculate  $b$  and  $b_\tau$ . The Monte Carlo expectation of  $b$  thereby obtained is  $b_{MC} = 0.57 \pm 0.01$ .

The observed decay angular distribution of the pions after background subtraction and efficiency correction is shown in Fig. 10. Fitting this distribution with a function of the form  $1 + b_{meas} \cos^2 \vartheta$  yields  $b_{meas} = 0.57 \pm 0.12$ . This result is in good agreement with our Monte Carlo expectation for a vector-like coupling. Expressing the measured value of  $b_{meas}$  in terms of a 95% confidence interval, we find the range  $0.38 < b_{meas} < 0.8$  is allowed. These bounds correspond to  $b_\tau$  in the interval  $2.3 < b_\tau < 10$ . From this an allowed range for the population densities of the  $\rho$  helicity states ( $r_1$  for  $|H_\rho| = 1$  and  $r_0$  for  $H_\rho = 0$  with  $r_0 + r_1 = 1$ ) can be

derived independently of any assumption about the structure of the interaction. With  $r_0 = (b_\tau + 1)/(b_\tau + 2) \equiv L/(L + R)$  one finds  $0.77 < r_0 < 0.92$  at 95% CL, indicating that neither of the  $\rho$  helicity states is exclusively populated.

This measurement can also be used to demonstrate that the  $\nu_\tau$  spin is  $J_{\nu_\tau} = \frac{1}{2}$ , if the  $\nu_\tau$  is assumed to be massless. The present best limit on the  $\nu_\tau$  mass is  $m_{\nu_\tau} < 35 \text{ MeV}/c^2$  at 95% CL.<sup>15</sup> The spins of the  $\rho$  and the  $\tau$  are known to be  $J_\rho = 1$  and  $J_\tau = \frac{1}{2}$ . No angular momentum transfer to the  $\rho \nu_\tau$  system can compensate the  $\nu_\tau$  spin, thus allowing only  $\nu_\tau$  spins of  $J_{\nu_\tau} = \frac{1}{2}$  and  $J_{\nu_\tau} = \frac{3}{2}$ . However,  $J_{\nu_\tau} = \frac{3}{2}$  requires the  $\rho$  helicity to be in a pure  $H_\rho = -1$  state, which is excluded by our measurement. Therefore, the spin of the  $\nu_\tau$  must be  $J_{\nu_\tau} = \frac{1}{2}$ .

### Conclusions

The mass of the  $\tau$  lepton has been measured, using a newly developed pseudomass method, to be:  $m_\tau = (1776.3 \pm 2.4 \pm 1.4) \text{ MeV}/c^2$ , representing the first evidence that the  $\tau$  mass is significantly lower than the previous world average. Indications of a possible violation of lepton universality become less significant using this lower  $\tau$  mass. Meanwhile the decrease in  $m_\tau$  has been confirmed by the more precise measurements of BES<sup>38</sup> and CLEO<sup>39</sup> of  $m_\tau = (1776.9_{-0.5}^{+0.4} \pm 0.2) \text{ MeV}/c^2$  and  $m_\tau = (1777.6 \pm 0.9 \pm 1.6) \text{ MeV}/c^2$ , respectively. In addition, new measurements on  $\tau_\tau$ ,  $B_e$  and  $B_\mu$  are available. Using the resulting new world averages of  $m_\tau = (1777.1 \pm 0.5) \text{ MeV}/c^2$ ,  $\tau_\tau = (295.7 \pm 3.2) \text{ fs}$ ,  $B_e = (17.76 \pm 0.15)\%$  and  $B_\mu = (17.53 \pm 0.19)\%$ <sup>40</sup> one finds:

$$\frac{g_\tau}{g_\mu} = 0.992 \pm 0.007,$$

which is in reasonable agreement with the Standard Model expectation.

Our measurement of  $m_\tau$  also leads to a revised upper limit on the mass of the  $\tau$  neutrino of  $m_{\nu_\tau} < 31 \text{ MeV}/c^2$  at the 95% confidence level. Note that the upper limit remains unchanged if the new world average for  $m_\tau$  is used.

In addition, a study of the decay  $\tau^- \rightarrow \pi^- \pi^0 \nu_\tau$  has been performed. The invariant mass spectrum of the  $\pi^- \pi^0$  final state has been shown, to agree well with the CVC prediction for this channel, suggesting that the  $\pi^- \pi^0$  system is produced in a  $J^P = 1^-$  state. The extraction of the pure  $\rho$  contribution is only possible using model assumptions,<sup>27</sup> e.g., radial excitations such as the  $\rho'$  or the opening of a new channel above the  $4\pi$  and  $\omega\pi$  threshold.

Since any possible deviations are small, we consider the decay  $\tau^- \rightarrow \pi^- \pi^0 \nu_\tau$  to be identical with the decay  $\tau^- \rightarrow \rho^- \nu_\tau$ . Our measurement of the branching ratio,  $\text{Br}(\tau^- \rightarrow \pi^- \pi^0 \nu_\tau) = (22.6 \pm 0.4 \pm 0.9)\%$ , agrees well with the world average of  $(23.01 \pm 0.55)\%$ . Note that the measurement reported here uses a new method,

which is largely independent of other tau branching ratios. Using our recent measurement of the electron branching ratio,  $\text{Br}(\tau^- \rightarrow e^- \bar{\nu}_e \nu_\tau) = (17.3 \pm 0.4 \pm 0.5)\%$ ,<sup>6</sup> we obtain:

$$\frac{\text{Br}(\tau^- \rightarrow \rho^- \nu_\tau)}{\text{Br}(\tau^- \rightarrow e^- \bar{\nu}_e \nu_\tau)} = 1.31 \pm 0.06,$$

where common systematic errors cancel in the ratio. The result is in good agreement with the recent theoretical predictions from Kühn and Santamaria of  $1.32 \pm 0.05$ ,<sup>27</sup> derived using CVC.

From the analysis of the angular distributions of the pions relative to the direction of flight of the  $\rho$  it follows that the  $\rho$  helicity state  $H_\rho = 0$  is favoured over  $|H_\rho| = 1$ , in the ratio expected from the Standard Model. The measurement of the polarization of  $\tau$  leptons produced in  $Z^0$  decays using the decay  $\tau^- \rightarrow \rho^- \nu_\tau$  is based on this behaviour; our result now justifies this procedure. With the assumption that the  $\nu_\tau$  is massless, the  $\nu_\tau$ -spin has been shown to be  $J_{\nu_\tau} = \frac{1}{2}$ , which is in agreement with the Standard Model.

## References

1. ARGUS Collab.: H. Albrecht et al., *Z. Phys. C* **55** (1992) 179.
2. MARK II Collab.: K.G. Hayes et al., *Phys. Rev. D* **25** (1982) 2869.
3. ARGUS Collab.: H. Albrecht et al., *Phys. Lett. B* **185** (1987) 228.
4. Crystal Ball Collab.: S. Keh et al., *Phys. Lett. B* **212** (1988) 123.
5. CLEO Collab.: T. Bowcock et al., *Phys. Rev. D* **41** (1990) 805.
6. ARGUS Collab.: H. Albrecht et al., *Z. Phys. C* **53** (1992) 367.
7. ARGUS Collab.: H. Albrecht et al., *DESY 92-125* (1992), submitted to *Z. Phys. C*.
8. N. Isgur, C. Morningstar and C. Reader, *Phys. Rev. D* **39** (1989) 1357.
9. ARGUS Collab.: H. Albrecht et al., *Phys. Lett. B* **250** (1990) 164.
10. T.N. Truong, *Phys. Rev. D* **30** (1984) 1509;  
F.J. Gilman and S.H. Rhie, *Phys. Rev. D* **31** (1985) 1066.
11. W.J. Marciano and A. Sirlin, *Phys. Rev. Lett.* **61** (1988) 1815.
12. Particle Data Group, K. Hikasa et al., *Phys. Rev. D* **45** (1992) 1.
13. D.I. Britton et al., *Phys. Rev. Lett.* **68** (1992) 3000.
14. E. Ma, S. Pakvasa and S.F. Tuan, *Part. World* **3** (1992) 27.
15. ARGUS Collab.: H. Albrecht et al., *Phys. Lett. B* **202** (1988) 149.
16. DELCO Collab.: W. Bacino et al., *Phys. Rev. Lett.* **41** (1978) 13.
17. A.A. Zholents et al., *Phys. Lett. B* **96** (1980) 214.
18. ARGUS Collab.: H. Albrecht et al., *Z. Phys. C* **33** (1986) 7.
19. D.P. Barber et al., *Phys. Lett. B* **135** (1984) 498.
20. ARGUS Collab.: H. Albrecht et al., *Nucl. Instr. Meth.* **A275** (1989) 1.
21. ARGUS Collab.: H. Albrecht et al., *Phys. Lett. B* **292** (1992) 221.
22. S. Jadach and Z. Was, *Comp. Phys. Commun.* **64** (1991) 267;  
S. Jadach, J.H. Kühn, and Z. Was, *Comp. Phys. Commun.* **64** (1991) 275.

23. ARGUS Collab.: H. Albrecht et al., *Z. Phys. C* **41** (1988) 405.
24. T. Sjöstrand, *Comp. Phys. Commun.* **39** (1986) 347;  
T. Sjöstrand and M. Bengtsson, *Comp. Phys. Commun.* **43** (1987) 367.
25. ARGUS Collab.: H. Albrecht et al., *Phys. Lett. B* **163** (1985) 404.
26. M.V. Danilov, in the Proceedings of the Joint International Lepton-Photon Symposium & Europhysics Conference on High Energy Physics, Geneva, Switzerland, 1991; edited by S. Hegarty, K. Porter, E. Quercigh, World Scientific, Singapore, (1992) and ITEP preprint ITEP-9-92 (1992).
27. J.H. Kühn and A. Santamaria, *Z. Phys. C* **48** (1990) 445.
28. ALEPH Collab.: D. Decamp et al., *Phys. Lett. B* **265** (1991) 430.
29. ARGUS Collab.: H. Albrecht et al., DESY 92-082 (1992), accepted by *Z. Phys. C*.
30. ARGUS Collab.: H. Albrecht et al., *Phys. Lett. B* **217** (1989) 205.
31. Particle Data Group, J.H. Hernández et al., *Phys. Lett. B* **239** (1990) 1.
32. R.D. Appuhn, Doctoral Thesis, Universität Dortmund (1992).
33. The value of  $(7.9 \pm 0.5)\%$  has been determined from the branching ratio for decays of the type  $\tau^- \rightarrow h^- \pi^0 \pi^0 \nu_\tau$  of  $(8.27 \pm 0.47)\%$ ,<sup>26</sup> where  $h$  stands for  $\pi$  or  $K$ , after a 0.4% correction for the contribution from  $K$  mesons.
34. Y.S. Tsai, *Phys. Rev. D* **4** (1971) 2821.
35. G. Gounaris and J.J. Sakurai, *Phys. Rev. Lett.* **21** (1968) 244.
36. B. Costa de Beauregard et al., *Phys. Lett. B* **67** (1977) 213;  
DM1 Collab.: A. Quenzer et al., *Phys. Lett. B* **76** (1978) 512.
37. A. Donnachie and H. Mirzaie, *Z. Phys. C* **33** (1987) 407;  
DM2 Collab.: D. Bisello et al., *Phys. Lett. B* **220** (1989) 321.
38. BES Collab.: J.Z. Bai et al., SLAC-PUB-5870 (1992).
39. B. Heltsley, these proceedings.
40. M. Davier, Summary Talk of the Second Workshop on Tau Lepton Physics, Columbus, Ohio, USA, September 1992.